



# NEW RESULTS IN DIFFRACTIVE PHOTOPRODUCTION FROM E687 AT FNAL

A. ZALLO

on behalf of the E687 Collaboration \*

Laboratori Nazionali di Frascati dell'INFN - via E. Fermi 40, Frascati I-00044

## Abstract

A narrow dip structure has been observed at  $1.9 \text{ GeV}/c^2$  in a study of diffractive photoproduction of the  $3\pi^+3\pi^-$  final state performed by the Fermilab experiment E687. Preliminary results on new structures in  $2\pi^+2\pi^-$  final states are also given.

## 1 INTRODUCTION

The Fermilab Experiment 687 collaboration has collected a large sample of high-energy photoproduction events, recorded with the E687 spectrometer [2][3] during the 1990/91 fixed-target runs at the Wideband Photon beamline at Fermilab. Although the experiment is focussed on charm physics, a very large sample of diffractively photoproduced light-meson events was also recorded. This paper reports on a study[1] of the diffractive photoproduction of the  $3\pi^+3\pi^-$  final state and the observation of a narrow dip in the mass spectrum at  $1.9 \text{ GeV}/c^2$ .

Preliminary results on diffractive photoproduction of  $2\pi^+2\pi^-$  final states are also shown.

## 2 E687 SPECTROMETER

In E687, a forward multiparticle spectrometer is used to measure the interactions of high-energy photons on a 4-cm-thick Be target. It is a large-aperture, fixed-target spec-

trometer with excellent vertexing, particle identification, and reconstruction capabilities for photons and  $\pi^0$ 's. The photon beam is derived from the Bremsstrahlung of secondary electrons of  $\approx 300 \text{ GeV}$  endpoint energy, which were produced by the  $800 \text{ GeV}/c$  Tevatron proton beam. The charged particles emerging from the target are tracked by a system of twelve planes of silicon microstrip detectors arranged in three views. These provide high-resolution separation of primary (production) and secondary (charm decay or interaction) vertices. The momentum of a charged particle is determined by measuring its deflections in two analysis magnets of opposite polarity with five stations of multiwire proportional chambers. Three multicell threshold Čerenkov counters are used to discriminate between pions, kaons, and protons. Photons and neutral pions are reconstructed by electromagnetic (EM) calorimetry. Hadron calorimetry and muon detectors provide triggering and additional particle identification.

## 3 EVENT SELECTION

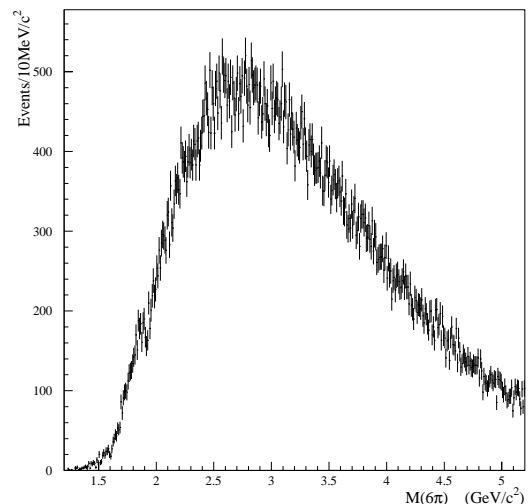


Figure 1: Distribution of  $3\pi^+3\pi^-$  invariant mass after applying a cut on the total energy deposited in the calorimeters with respect to the total energy in the spectrometer.

Pions are produced in photon interactions in the Be target. The data acquisition trigger requires a minimum en-

\* co authors: P.L. Frabetti (INFN and Bologna); H.W.K. Cheung, J.P. Cumalat, C. Dallapiccola, J.F. Ginkel, W.E. Johns, M.S. Nehring, E.W. Vaandering (UC Boulder); J.N. Butler, S. Cihangir, I. Gaines, P.H. Garbincius, L. Garren, S.A. Gourlay, D.J. Harding, P. Kasper, A. Kreymer, P. Lebrun, S. Shukla, M. Vittoni (Fermilab); R. Baldini-Ferroli, S. Bianco, F.L. Fabbri, S. Sarwar (INFN Frascati); C. Cawfield, R. Culbertson, R.W. Gardner, E. Gottschalk, R. Greene, K. Park, A. Rahimi, J. Wiss (UI Champaign); G. Alimonti, G. Bellini, M. Boschini, D. Brambilla, B. Caccianiga, L. Cinquini, M. DiCorato, P. Dini, M. Giannini, P. Inzani, F. Leveraro, S. Malvezzi, D. Menasce, E. Meroni, L. Milazzo, L. Moroni, D. Pedrini, L. Perasso, F. Prelz, A. Sala, S. Sala, D. Torretta (INFN and Milano); D. Buchholz, D. Claes, B. Gobbi, B. O'Reilly (Northwestern); J.M. Bishop, N.M. Cason, C.J. Kennedy, G.N. Kim, T.F. Lin, D.L. Pusejlic, R.C. Ruchti, W.D. Shephard, J.A. Swiatek, Z.Y. Wu (Notre Dame); V. Arena, G. Boca, G. Bonomi, C. Castoldi, G. Gianini, M. Merlo, S.P. Ratti, C. Riccardi, L. Viola, P. Vitulo (INFN and Pavia); A.M. Lopez, L. Mendez, A. Mirles, E. Montiel, D. Olaya, J.E. Ramirez, C. Rivera, Y. Zhang (Mayaguez, Puerto Rico); J.M. Link, V.S. Paolone, P.M. Yager (UC DAVIS); J.R. Wilson (USC Columbia); J. Cao, M. Hosack, P.D. Sheldon (Vanderbilt); F. Davenport (UNC Asheville); K. Cho, K. Danyo, T. Handler (UT Knoxville); B.G. Cheon, Y.S. Chung, J.S. Kang, K.Y. Kim, K.B. Lee, S.S. Myung (Korea University, Seoul)

ergy deposition in the hadron calorimeters located behind the electromagnetic calorimeters and at least three charged tracks outside the pair region. The microstrip system and the forward spectrometer measure the six-pion final state (in this paper,  $6\pi$  refers to the  $3\pi^+3\pi^-$  state) with a mass resolution  $\sigma = 10 \text{ MeV}/c^2$  at a total invariant mass of about  $2 \text{ GeV}/c^2$ . It is required that a single six-prong vertex be reconstructed in the target region by the microstrip detector, with a good confidence level. Such a requirement rejects background due to secondary interactions in the target. Exclusive final states are selected by also requiring that the same number of tracks be reconstructed in the magnetic spectrometer. The six microstrip tracks and the six spectrometer tracks are required to be linked, with no ambiguity in associating the microstrip and spectrometer tracks. Events with particles identified by the Čerenkov system as definite electrons, kaons, or protons, or as kaon/proton ambiguous are eliminated and at least four out of six particles have to be positively identified as  $\pi^\pm$ . Particle identification is tested by assuming that one or two out of the six tracks is a  $K^\pm$ , by computing all two-track invariant mass combinations, and verifying that there is no evidence of a peak at the  $K^*$  or at the  $\phi$  mass. We eliminated final states with  $\pi^0$ 's by rejecting events with visible energy in the electromagnetic calorimeters that was not associated with the charged tracks. A cut in this variable ( $E_{\text{cal}}/E_{6\pi} \leq 5\%$ ) is applied on the calorimetric neutral energy normalized to the six-pion energy measured in the spectrometer. The distribution of the six-pion invariant mass after these cuts is shown in Fig. 1. The plot shows a structure at  $1.9 \text{ GeV}/c^2$ . In the following, only the  $6\pi$  mass region around this structure will be analyzed.

For diffractive reactions at our energies, the square of the four-momentum transfer  $t$  can be approximated by the square of the total transverse momentum  $P_T^2$  of the diffractively produced hadronic final state. Using this definition, the  $P_T^2$  distribution of diffractive events, Fig. 2, is well described by two exponentials: a coherent contribution with a slope  $b_c = 54 \pm 2 \text{ (GeV}/c)^{-2}$  consistent with the Be form factor [4] and an incoherent contribution with a slope  $b_i = 5.10 \pm 0.25 \text{ (GeV}/c)^{-2}$ .

Taking only events with  $P_T^2 \leq 0.040 \text{ GeV}^2/c^2$ , we evaluated a contamination of about 50% from nondiffractive events. This incoherent contribution shows no structure in the  $1.2\text{--}3.0 \text{ GeV}/c^2$  mass range, Fig. 3. The diffractive mass distribution was obtained by subtracting this contribution, parametrized by a polynomial fit, and dividing the yield by the detection efficiency.

The detection efficiency was computed by modeling diffractive photoproduction of a mass  $M$ , using the experimentally found slope  $b_c$ , and simulating the decay  $M \rightarrow 6\pi$  according to phase space [5]. There is no threshold or discontinuity for the efficiency, particularly in the region of the dip structure. At  $1.9 \text{ GeV}/c^2$ , the (self-normalized relative) efficiency  $A$  varied as  $dA/A/dM_{6\pi} = 0.15/\text{GeV}/c^2$ . The efficiency and the efficiency-corrected distribution of the six-pion invariant mass for diffractive events, in the

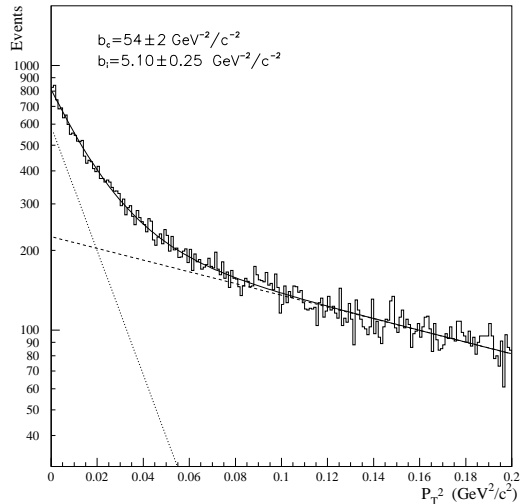


Figure 2: Transverse momentum squared distribution showing the diffractive peak.

mass range  $1.4\text{--}2.4 \text{ GeV}/c^2$ , are shown in Fig. 4. There is no evidence, albeit with large combinatorial backgrounds, for resonance substructure, e.g.,  $\rho^0 \rightarrow \pi^+\pi^-$ , in the  $6\pi$  data below  $M_{6\pi} = 2.0 \text{ GeV}/c^2$ , either at the mass region of the dip or in nearby sidebands. Similarly, the efficiency or acceptance exhibited no threshold, edge, or discontinuity over the entire mass region observed, when the six pion state was simulated as a sequence of decays of intermediate two-body resonances, for example  $a_1^+ + a_1^- \rightarrow (\rho^0\pi^+) + (\rho^0\pi^-) \rightarrow (\pi^+\pi^-\pi^+) + (\pi^+\pi^-\pi^-)$ , even under extreme assumptions of full longitudinal or transverse polarizations for the initial state.

The presence of a dip at  $1.9 \text{ GeV}/c^2$  was verified by several systematic checks. Diffractive photoproduction of  $D^0\bar{D}^0$  pairs or the associated production of  $\bar{D}^0$  plus a charm baryon at low  $t$  (where the decay products of the other charm meson or charm baryon are missed) followed by the  $6\pi$  decay of the  $D^0$  or  $\bar{D}^0$  are estimated by Monte Carlo simulation to be negligible contributions. It was also checked that demanding more stringent cuts (i.e., requiring that all six particles be identified as  $\pi^\pm$ , applying a sharper cut on the calorimeter neutral energy, or subtracting the incoherent contribution bin by bin) increases the statistical errors without significantly affecting the behavior shown in Fig. 3.

A three-parameter polynomial fit was performed, solid line in Fig. 4, to explore the hypothesis that any structure in this distribution is a statistical fluctuation. The normalized residual distribution, evaluated for each  $10\text{-MeV}/c^2$  bin, is good in the full invariant mass range, with the exception of the interval centered at  $1.9 \text{ GeV}/c^2$ , the region of the claimed dip, where a poor  $\sim 10^{-3}$  confidence level interval, is obtained, making it highly unlikely that the observed dip is a statistical fluctuation. Incoherently adding a Breit-

Wigner to the fit does not improve the fit quality much.

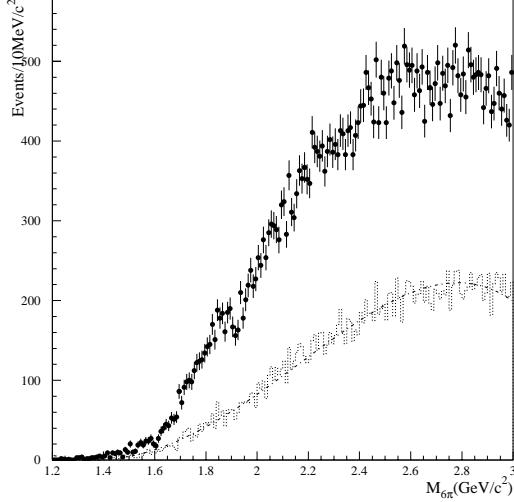


Figure 3: Distribution of  $3\pi^+3\pi^-$  invariant mass in the 1.2–3.0  $\text{GeV}/c^2$  mass range: coherent plus incoherent contribution. Dotted distribution: incoherent contribution.

#### 4 FITTING THE SIX-PION INVARIANT MASS DISTRIBUTION

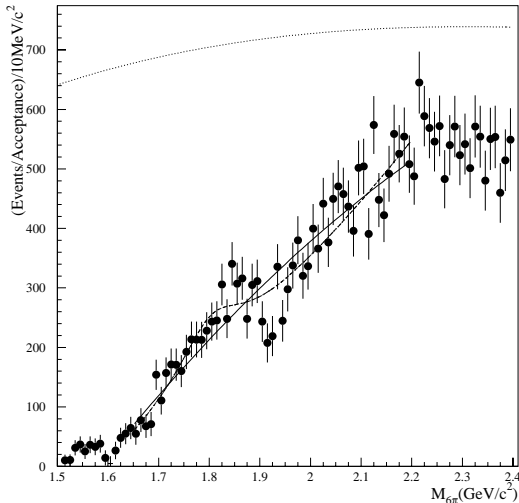


Figure 4: Acceptance-corrected distribution of  $3\pi^+3\pi^-$  invariant mass for diffractive events after subtracting incoherent contribution. Solid line: second-order polynomial fit. Dashed line: polynomial fit with incoherently-added Breit-Wigner. Upper dot line: relative detection efficiency (arbitrary normalization).

Because of the narrow width, the E687 spectrometer mass resolution,  $\sigma = 10 \text{ MeV}/c^2$  at  $2 \text{ GeV}/c^2$ ,

was unfolded by applying the method described in Ref. [6]: the experimentally observed data distribution  $r(x)$  and the unfolded mass distribution  $a(x)$  are related by  $a(x) \sim r(x) - 0.5\sigma^2 \cdot r(x)''$ , where  $r(x)''$  is the second derivative with respect to  $M_{6\pi}$  for the observed distribution. This relationship results from applying a Fourier transform and approximating the resolution function by  $g(x) = \exp(-\frac{\sqrt{2}|x|}{\sigma})$ , which is marginally different from a Gaussian. A fit similar to the following one is used to obtain  $r(x)''$  from the unfolded data. The data after unfolding are shown in Fig. 5.

The dip structure at  $1.9 \text{ GeV}/c^2$  has been characterized by a two-component fit, adding coherently a relativistic Breit-Wigner resonance to a diffractive continuum contribution. The continuum probability distribution  $F_{JS}(M)$  has been modeled after a Jacob-Slansky diffractive parameterization[7], plus a constant term  $c_0$

$$F_{JS}(M) = f_{JS}^2(M) = c_0 + c_1 \frac{e^{\frac{-\beta}{M-M_0}}}{(M-M_0)^{2-\alpha}}$$

The Jacob-Slansky amplitude  $f_{JS}(M)$  is assumed to be the purely real ( $\phi_{JS} \equiv 0$ ) square root of the probability function  $F_{JS}(M)$ . For the fit, a relative phase factor  $e^{i\phi}$ , independent of mass, and a normalizing factor  $a_r$  multiplied a relativistic Breit-Wigner resonance term, giving the overall amplitude

$$A(M) = f_{JS}(M) + a_r \frac{-M_r \Gamma e^{i\phi}}{M^2 - M_r^2 + iM_r \Gamma}$$

Fit results are shown in Table 1 and in Fig. 5 for a fitted mass range from 1.65 to 2.15  $\text{GeV}/c^2$ , symmetric with respect to the dip. Quantities shown are the mass and width of the resonance, the amplitude ratio  $a_r/f_{JS}(M_r)$  between the Breit-Wigner function and the Jacob-Slansky continuum, the relative phase and the  $\chi^2/\text{dof}$ . Fit values show consistent evidence for a narrow resonance at  $M_r = 1.911 \pm 0.004 \pm 0.001 \text{ GeV}/c^2$  with a width  $\Gamma = 29 \pm 11 \pm 4 \text{ MeV}/c^2$ , where the errors quoted are statistical and systematic, respectively. The fit values shown in Fig. 5 and represented by the parameters of Table 1 are stable with acceptable  $\chi^2/\text{dof}$  over varying mass ranges from 1.65 to 2.3  $\text{GeV}/c^2$ . We quote as systematic error the sample variance of the fit values due to our choice of fit mass range. The quality of the fit deteriorates somewhat as the upper limit of the fit for this simple model is extended from 2.1 to 3.0  $\text{GeV}/c^2$ . However, the only fit parameter that is affected is the width, which varies from  $29 \pm 11 \text{ MeV}/c^2$  to  $40 \pm 20 \text{ MeV}/c^2$ .

#### 5 DIFFRACTIVE PHOTOPRODUCTION OF $2(\pi^+\pi^-)$ EVENTS

About one million of  $2(\pi^+\pi^-)$  events have been recorded by E687 in the 1990/91 fixed target runs at the Fermi National Accelerator Laboratory. Their analysis is in progress

Table 1: Fit results for a mass range from 1.65 to 2.15  $GeV/c^2$

$M_r$ ( $GeV/c^2$ )	$1.911 \pm 0.004$
$\Gamma$ ( $MeV/c^2$ )	$29 \pm 11$
$a_r/f_{JS}(M_r)$	$0.31 \pm 0.07$
$\phi$ (deg.)	$62 \pm 12$
$\chi^2/dof$	1.1

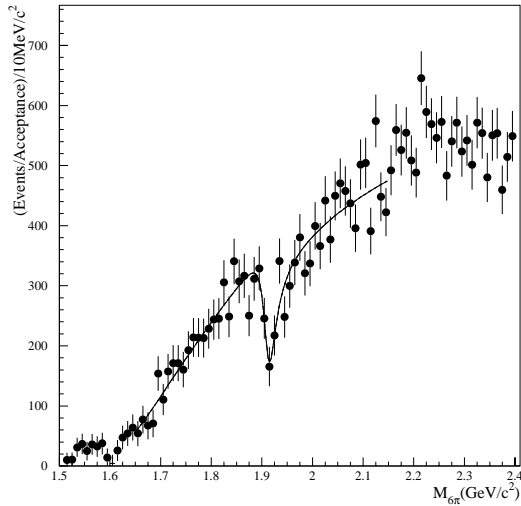


Figure 5: Acceptance-corrected distribution of  $3\pi^+3\pi^-$  invariant mass for diffractive events. The mass resolution has been unfolded. Fit parameters are listed in Table 1.

and in the following only a preliminary presentation is given. As in the  $3\pi^+3\pi^-$  study, exclusive final states are selected based on the total number of charged tracks seen in the spectrometer and final states with  $\pi^0$ 's are rejected by requiring no visible energy in the electromagnetic calorimeters. The particle identification has been done applying the same cuts described in section 3. The t-distribution shows a  $P_T^2$  slope of about  $60 (GeV/c)^{-2}$ , in good agreement with the  $3\pi^+3\pi^-$  sample. Taking only events with  $P_T^2 \leq 0.0625 GeV^2/c^2$ , our  $2(\pi^+\pi^-)$  sample remains with a contamination of about 25% from non-diffractive events.

The acceptance corrected  $2(\pi^+\pi^-)$  mass spectrum is shown in Fig. 6(top). Although we expect, to first order, that the bump in the mass spectrum below  $2.0 GeV/c^2$  is dominated by the  $\rho(1450)$  vector meson, our fit is not good (solid line) even when we add 3 P-Wave interfering Breit-Wigner: the  $\chi^2$  is 467.0 for 274 degrees of freedom. As the acceptance is almost flat for  $M_{4\pi} \sim 1.6 GeV^2/c^2$ , the deviations observed should be of physical origin. The residuals (data - fitted values) shown in Fig. 6(bottom) clearly show structures with a non negligible statistical significance. Their study is in progress. For the time being we can say that the

ratio of the residuals to the total yield in  $4\pi$  is of the same order of the  $\rho - \omega$  mixing effect in  $2\pi$ [8], shown in Fig. 7.

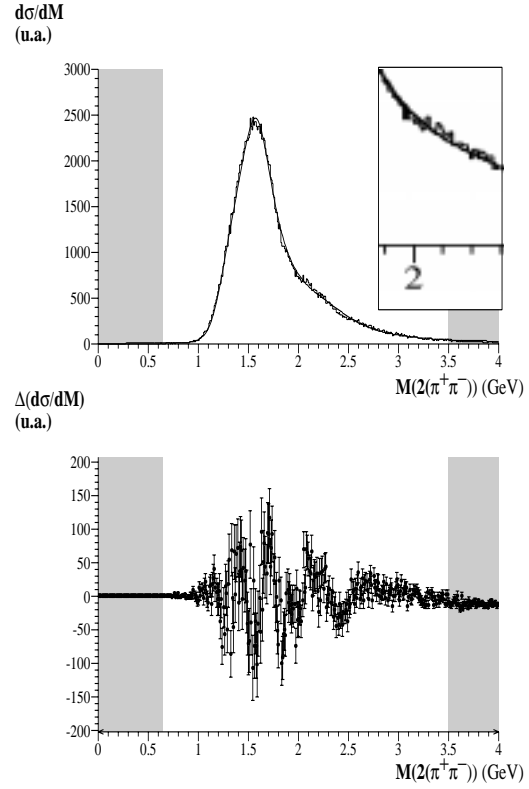


Figure 6: Acceptance corrected  $2(\pi^+\pi^-)$  mass (top) and residual (data - fitted values) distributions (bottom). The solid line is the 3 P-Wave Breit-Wigner fit.

## 6 CONCLUSIONS

The diffractive photoproduction of  $3\pi^+3\pi^-$  has been studied by E687. Evidence has been found for a narrow structure near  $M_{6\pi} = 1.9 GeV/c^2$ . If this dip is characterized as the destructive interference of a resonance with the continuum background, then the parameters of this resonance would be  $M_r = 1.911 \pm 0.004 \pm 0.001 GeV/c^2$ , with  $\Gamma = 29 \pm 11 \pm 4 MeV/c^2$ . Such a resonance could be assigned the photon quantum numbers ( $J^{PC} = 1^{--}$ ) and  $G=+1, I=1$  due to the final state multiplicity.

The possible presence of other structures in the  $2(\pi^+\pi^-)$  final state needs further study.

## 7 REFERENCES

- [1] P. L. Frabetti *et al.* (E687 Coll.), hep-ex/0106029.
- [2] P.L. Frabetti *et al.* (E687 Coll.), Nucl. Instrum. Meth. A **320**, 519 (1992).

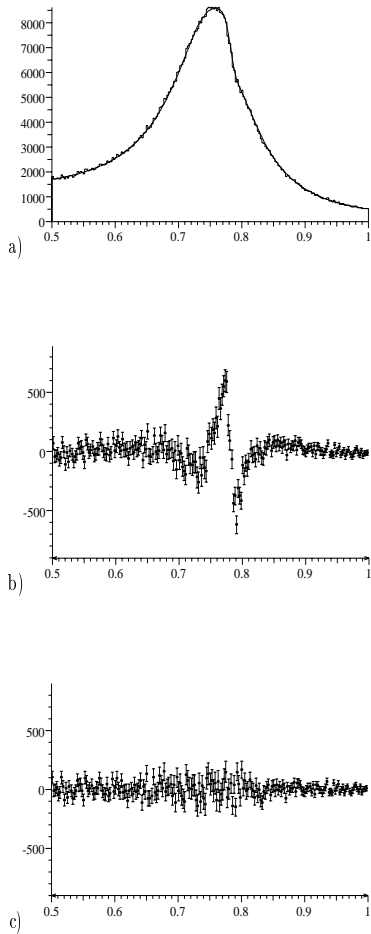


Figure 7: a- the  $M_2\pi$  spectrum in the range 0.5-1.0  $\text{GeV}/c^2$ , around the  $\rho(770) - \omega(783)$  pole mass (top); b- residual (fit-data) once the mixing amplitude is fixed to 0; c- residuals (fit-data) when the interfering amplitude is included.

- [3] P.L. Frabetti *et al.* (E687 Coll.), Nucl. Instrum. Meth. A **329**, 62 (1993).
- [4] C.W. De Jager, H. De Vries, and C. De Vries, Atom. Data and Nucl. Data Tables **36** (1987) 495.
- [5] F. James, GENBOD N-Body Monte-Carlo Event Generator, CERN Computer Centre Program Library.
- [6] E. Sjøntoft, Nucl. Instrum. Meth. **163** (1979) 519.
- [7] M. Jacob and R. Slansky, Phys. Lett. B **37** (1971) 408, and Phys. Rev. D **5** (1972) 1847.
- [8] P.L. Frabetti *et al.* (E687 Coll.), EPS-HEP97, Jerusalem, 19-26 august (1993).